

New shapes of light-cone distributions of the transversely polarized ρ -mesons

A.P. Bakulev^a, S.V. Mikhailov^b

Bogolyubov Lab. of Theoretical Physics, Joint Institute for Nuclear Research, 141980, Moscow Region, Dubna, Russia

Received: 20 October 2000 / Published online: 15 March 2001 – © Springer-Verlag 2001

Abstract. The leading twist light-cone distributions for transversely polarized ρ -, ρ' - and b_1 -mesons are re-analyzed in the framework of QCD sum rules with nonlocal condensates. Using different kinds of sum rules to obtain reliable predictions, we estimate the 2nd, 4th, 6th and 8th moments for transversely polarized ρ - and ρ' -meson distributions and re-estimate the tensor couplings f_{ρ, ρ', b_1}^T . We stress that the results of the standard sum rules also support our estimate of the second moment of the transversely polarized ρ -meson distribution. New models for light-cone distributions of these mesons are constructed. Phenomenological consequences of these distributions are briefly discussed. Our results are compared with those found by Ball and Braun in 1996, and the latter are shown to be incomplete.

1 Introduction

In this paper, we complete our investigation of the leading twist light-cone distribution amplitudes (DAs) for the lightest transversely polarized mesons with quantum numbers $J^{PC} = 1^{--}$ (ρ_\perp , ρ'_\perp), 1^{+-} ($b_{1\perp}$) in the framework of QCD sum rules (SRs) with nonlocal condensates (NLCs). These DAs are important ingredients of the “factorization” formalism [1] for any hard exclusive reactions involving ρ -mesons. For this reason, the DAs have been attractive for theorists for a long time: the main points are presented in [2,3]; a detailed revised version of the standard approach is in [4], and a generalization to the next twists is in [5]. The leading twist DA $\varphi_{\rho, \rho', b_1}^T(x, \mu^2)$ parameterizes the matrix elements of the tensor current with transversely polarized $\rho(770)$ - and $\rho'(1465)$ -mesons ($J^{PC} = 1^{--}$):

$$\begin{aligned} & \langle 0 | \bar{u}(z) \sigma_{\mu\nu} d(0) | \rho_\perp(p, \lambda) \rangle \Big|_{z^2=0} \\ &= i f_{\rho_\perp}^T (\varepsilon_\mu(p, \lambda) p_\nu \\ & - \varepsilon_\nu(p, \lambda) p_\mu) \int_0^1 dx e^{ix(zp)} \varphi_{\rho_\perp}^T(x, \mu^2) + \dots, \end{aligned} \quad (1)$$

and the $b_1(1235)$ -meson ($J^{PC} = 1^{+-}$):

$$\begin{aligned} & \langle 0 | \bar{u}(z) \sigma_{\mu\nu} d(0) | b_1^+(p, \lambda) \rangle \Big|_{z^2=0} \\ &= f_{b_1}^T \epsilon_{\mu\nu\alpha\beta} \varepsilon^\alpha(p, \lambda) p^\beta \int_0^1 dx e^{ix(zp)} \varphi_{b_1}^T(x, \mu^2) \\ &+ \dots \end{aligned} \quad (2)$$

(here dots represent higher-twist contributions, explicitly defined in Appendix A, see (A.9) and (A.10) and [5]). In the above definitions, p_ν and $\varepsilon_\mu(p, \lambda)$ are the momentum and the polarization vector of a meson, respectively, and μ^2 is normalization point.

In the framework of the standard approach, one should restrict oneself to an estimate of the second moment $\langle \xi^2 \rangle$ of the DA to restore its shape¹. In other words, the variety of different DA shapes is reduced to the 1-parameter family of “admissible” DAs:

$$\varphi(x; a_2) = 6x(1-x) \left[1 + a_2 C_2^{3/2} (2x-1) \right].$$

This family includes both the asymptotic DA ($a_2 = 0$) and the Chernyak–Zhitnitsky model [2] for the pion DA ($a_2^{\pi|CZ} = -2/3$). For the pion case, one might think it is rather enough: most of the debates (see [2, 6, 10–12] and references therein) about the shape of this DA are concerned just with the value of the coefficient a_2 – is it close to 0 or to $a_2^{\pi|CZ}$? In our opinion, advocated since 1986 [6], the shape of the pion DA is not far from the asymptotic one [6, 7, 13, 14, 8]. Only recently, researchers have tried to extract the next Gegenbauer coefficient [12] and other parameters of the pion DA [15] from experimental data. But, in general, there is no principle to exclude a more rich structure for a hadron DA. In this case, the standard approach is definitely out of its applicability range, and one should use more refined techniques, e.g., the QCD SRs with NLC.

This work was started in [8] where the “mixed parity” NLC SR for DAs of ρ - and b_1 -mesons, the particles pos-

¹ We should note in this respect that the standard approach could not provide a reliable estimate even for the second moment of DA, see [6–9]

^a e-mail: bakulev@thsun1.jinr.ru

^b e-mail: mikhs@thsun1.jinr.ru

sessing different P-parities, was analyzed. We concluded that, to obtain a reliable result, one should reduce the model uncertainties due to the nonlocal gluon contribution. Separate SRs for each P -parity channel should be preferable for this purpose, and here we construct these “pure parity” SRs for the corresponding DAs. The SR of this type possesses a low sensitivity to the gluon model but involves contributions from higher twists². To construct a refined “pure parity” SR for twist 2 DA, one must resolve the corresponding system of equations (see Appendix A). We realize this solution using the duality transformation, introduced in our previous work [16]. The negative parity NLC SR for the transversely polarized ρ -, ρ' -mesons works rather well and allows us to estimate the 2nd, 4th, 6th, and 8th moments of the leading twist DAs. The positive parity SR for the transversely polarized b_1 -meson can provide only the value of the b_1 -meson tensor coupling, $f_{b_1}^T$. We suggest the models for these DAs and check their self-consistency, based upon both “pure” and “mixed” NLC SR. The DA shape $\varphi_{\rho\perp}^T(x)$ differs noticeably from the known one. Finally, we inspect how these models can influence the $B \rightarrow \rho e \nu$ decay form factors.

The approach has been grounded in [6, 7, 17]; the calculation technique is the same as in [7, 8]. Therefore, the corresponding details are omitted below. Some important features of the NLC SRs approach should briefly be recalled.

The original tools of NLC SR are nonlocal objects like $M_S(z^2) = \langle \bar{q}(0)E(0, z)q(z) \rangle^3$ or $M_V^\mu(z) = \langle \bar{q}(0)\gamma^\mu E(0, z)q(z) \rangle$, rather than constant quantities of $\langle \bar{q}(0)q(0) \rangle$ type. Note that, in deriving the sum rules, one can always make a Wick rotation and treat all the coordinates as Euclidean: $z^2 = -\tilde{z}_{\text{Eucl}}^2 < 0$. The NLC $M_S(z^2)$ can be expanded in the Taylor series over the standard (local) condensates, $\langle \bar{q}(0)q(0) \rangle$, $\langle \bar{q}(0)\nabla^2 q(0) \rangle$, and over “higher dimensions” (see details of the expansion of different NLCs in [18]). We have

$$M_S(z^2) = \langle \bar{q}(0)q(0) \rangle - \frac{\tilde{z}^2}{8} \langle \bar{q}(0)\nabla^2 q(0) \rangle + \dots \quad (3)$$

So one can return to the standard SR by truncating this series. But, in virtue of the cut-off, one loses an important physical property of the nonperturbative vacuum – the possibility of vacuum quarks (gluons) to flow through vacuum with a nonzero momentum $k_{q(g)} \neq 0$. The parameter $\langle k_q^2 \rangle$, fixing the average virtuality of vacuum quarks, can be interpreted as a measure of condensate “nonlocality” λ_q^2 ,

$$\langle k_q^2 \rangle = \lambda_q^2 = \frac{\langle \bar{q}(0)\nabla^2 q(0) \rangle}{\langle \bar{q}(0)q(0) \rangle} = \frac{\langle \bar{q}(0) (ig\sigma_{\mu\nu}G^{\mu\nu}) q(0) \rangle}{2\langle \bar{q}(0)q(0) \rangle} \quad [\text{chiral limit}] .$$

The λ_q^2 was estimated from the mixed condensate of dimension 5, $\lambda_q^2 \approx 0.4\text{--}0.5 \text{ GeV}^2$ [19, 20]. It is important that

² As was noted in [4]

³ Here $E(0, z) = P \exp(i \int_0^z dt_\mu A_\mu^a(t)\tau_a)$ is the Schwinger phase factor required for gauge invariance

its value is of the order of the characteristic hadronic scale, $\lambda_q^2 \sim m_\rho^2 \approx 0.6 \text{ GeV}^2$; therefore the nonlocality effect can be large, and it should be taken into account in QCD SR. Really, the second term in the expansion (3) of $M_S(z^2)$ that is the inverse of the first one in sign becomes of the order of the first term at $|z^2| \sim 1/m_\rho^2$ due to the estimate $|\lambda_q^2 z^2| \sim 1$. Moreover, we should take into account the whole set of $(\lambda_q^2 z^2)^n$ -type corrections, appearing in the Taylor expansion. These corrections just mainly form the decay rate of the NLC ($M_S(z^2)$). The sensitivity to this rate is crucial for the DA moment SR: it leads to a much softer behavior of DA near the end points $x = 0, 1$ and allows one to extend QCD SR to higher moments $\langle \xi^N \rangle \equiv \int_0^1 \varphi(x)(2x-1)^N dx$, as was shown in [6].

Since neither QCD vacuum theory exists yet, nor higher dimension condensates are estimated, it is clear that merely the models of NLC can be suggested (Appendix B). Here we apply the simplest ansatz to NLC [7, 8] that takes into account only the main effect $\langle k_q^2 \rangle = \lambda_q^2 \neq 0$ and fixes the length of the quark–gluon correlations in the QCD vacuum: $\Lambda = 1/\lambda_q \approx 0.8 \text{ fm}$ [6, 7]. This suggestion leads to the simple Gaussian decay for $M_S(z^2)$, while the coordinate behavior of other NLCs looks more complicated. Certainly, the single scale of decay for all types of NLC (see Appendix B) looks as a crude model. But the model can be rather crude if one deals with SRs only for the first few moments $\langle \xi^N \rangle$, because for these integral characteristics the details of the NLC behavior do not appear to be very important (see the discussion in Sect. 5). An alternative case is provided by a special SR [13, 14] constructed directly for the shape of DAs.

Presently the lattice calculations of NLC provide inspiring knowledge [21, 22] for QCD SR. The latter measurement in [22] confirms the validity of the Gaussian ansatz for $M_S(z^2)$ (at a small distance) as well as the value of the parameter λ_q^2 .

2 “Duality” transformation

To obtain the sum rule, we start with the 2-point correlator $\Pi^{\mu\nu;\alpha\beta}(q)$ of the tensor currents $J_{(N)}^{\mu\nu}(x) = \bar{u}(x)\sigma^{\mu\nu}(z\nabla)^N d(x)$ (z is a light-like vector, $z^2 = 0$),

$$\Pi_{(N)}^{\mu\nu;\alpha\beta}(q) = i \int d^4x e^{iq \cdot x} \langle 0 | T [J_{(0)}^{\mu\nu+}(x) J_{(N)}^{\alpha\beta}(0)] | 0 \rangle, \quad (4)$$

whose properties were partially analyzed in [3, 4, 16]. It is well known that the correlator at $N = 0$ can be decomposed in invariant form factors Π_\pm , [3, 4]:

$$\Pi_{(0)}^{\mu\nu;\alpha\beta}(q) = \Pi_-(q^2)P_1^{\mu\nu;\alpha\beta} + \Pi_+(q^2)P_2^{\mu\nu;\alpha\beta}, \quad (5)$$

where the projectors $P_{1,2}$, obeying the projector-type relations

$$\begin{aligned} (P_i \cdot P_j)^{\mu\nu;\alpha\beta} &\equiv P_i^{\mu\nu;\sigma\tau} P_j^{\sigma\tau;\alpha\beta} = \delta_{ij} P_i^{\mu\nu;\alpha\beta} \\ &\quad (\text{no sum over } i), \\ P_i^{\mu\nu;\mu\nu} &= 3, \end{aligned} \quad (6)$$

are presented in Appendix A. For the general case $N \neq 0$, a similar decomposition involves four new independent tensors Q_i ; they appear due to a new vector z^α introduced into the composite tensor current operator,

$$\begin{aligned} \Pi_{(N)}^{\mu\nu;\alpha\beta}(q) &= \Pi_-(q^2, qz)P_1^{\mu\nu;\alpha\beta} + \Pi_+(q^2, qz)P_2^{\mu\nu;\alpha\beta} \\ &+ K_1(q^2, qz)Q_1^{\mu\nu;\alpha\beta} + K_3(q^2, qz)Q_3^{\mu\nu;\alpha\beta} \\ &+ K_z(q^2, qz)Q_z^{\mu\nu;\alpha\beta} + K_q(q^2, qz)Q_q^{\mu\nu;\alpha\beta}. \end{aligned} \quad (7)$$

The contributions of DAs, defined in (A.9) and (A.10), to the different tensor structures in the decomposition (7) are mixed, see (A.11) and (A.12). The most effective way to disentangle them in practical OPE calculations is to use explicit properties of different OPE terms under the duality transformation \hat{D} (introduced in our previous work [16]) mapping any rank-4 tensor $T^{\mu\nu;\alpha\beta}$ to another rank-4 tensor $T_D^{\mu\nu;\alpha\beta} = (\hat{D}T)^{\mu\nu;\alpha\beta}$ with

$$D_{\mu'\nu';\alpha'\beta'}^{\mu\nu;\alpha\beta} = \frac{-1}{4} \epsilon^{\mu\nu}{}_{\mu'\nu'} \epsilon_{\alpha'\beta'}{}^{\alpha\beta} \quad \text{and} \quad \hat{D}^2 = 1. \quad (8)$$

Our projectors $P_1^{\mu\nu;\alpha\beta}$, $P_2^{\mu\nu;\alpha\beta}$, $Q_1^{\mu\nu;\alpha\beta}$, $Q_3^{\mu\nu;\alpha\beta}$, $Q_z^{\mu\nu;\alpha\beta}$, and $Q_q^{\mu\nu;\alpha\beta}$ transform into each other under the action of \hat{D} :

$$\begin{aligned} (\hat{D}P_1)^{\mu\nu;\alpha\beta} &= P_2^{\mu\nu;\alpha\beta}, \\ (\hat{D}Q_1)^{\mu\nu;\alpha\beta} &= [P_1 + P_2 - Q_3]^{\mu\nu;\alpha\beta}, \end{aligned} \quad (9)$$

$$\begin{aligned} (\hat{D}P_2)^{\mu\nu;\alpha\beta} &= P_1^{\mu\nu;\alpha\beta}, \\ (\hat{D}Q_3)^{\mu\nu;\alpha\beta} &= [P_1 + P_2 - Q_1]^{\mu\nu;\alpha\beta}, \end{aligned} \quad (10)$$

$$(\hat{D}Q_z)^{\mu\nu;\alpha\beta} = -Q_z^{\mu\nu;\alpha\beta}, \quad (11)$$

$$(\hat{D}Q_q)^{\mu\nu;\alpha\beta} = [Q_q - Q_z + Q_1 + Q_3 - P_1 - P_2]^{\mu\nu;\alpha\beta}.$$

We have shown in [16] that all terms in OPE could be divided into two classes, a self-dual one ($\hat{D}X_{\text{SD}} = X_{\text{SD}}$) and an anti-self-dual one ($\hat{D}X_{\text{ASD}} = -X_{\text{ASD}}$). For example, the perturbative term is of ASD type, whereas the 4-quark scalar condensate contribution to OPE is of SD type.

Below we introduce the following shorthand notation for the contributions of DAs to the decomposition (7): v_0 , v_1 , and v_2 stand for 1^{--} (ρ_\perp , ρ'_\perp), and u_0 , u_1 , and u_2 , for 1^{+-} (b_1); see Appendix A for details. For the SD parts of OPE $u_i = -v_i$, and the system of equations simplifies to

$$\begin{aligned} \frac{\Pi_{\mp}(q^2, qz)}{2(qz)^N q^2} &= \mp v_0 - v_1 - v_2, \\ \frac{K_{1,3}(q^2, qz)}{2(qz)^N q^2} &= \mp v_1 + v_2, \\ \frac{K_q(q^2, qz) = -2K_z(q^2, qz)}{4(qz)^N q^2} &= v_2, \end{aligned} \quad (12)$$

whereas for the ASD parts $u_i = v_i$, and we have

$$\begin{aligned} \frac{\Pi_{\mp}(q^2, qz)}{2(qz)^N q^2} &= \mp v_0 + v_1 + v_2, \\ \frac{K_{1,3}(q^2, qz)}{2(qz)^N q^2} &= -v_1 - v_2, \\ \frac{K_z(q^2, qz)}{2(qz)^N q^2} &= +v_2, \\ K_q(q^2, qz) &= 0. \end{aligned} \quad (13)$$

By these formulas, it is possible to determine ρ - and b_1 -meson DA contributions of leading and higher twists.

3 The ‘‘mixed parity’’ sum rule

The usual way [2, 4] to extract the moments of the function $\varphi^{\text{T}}(x)$ appeals to the correlator $J_{(N,0)}(q^2)$ of the currents $J_{(N)}^{\mu\alpha}(0)z^\alpha$ and $J_{(0)}^{\mu\beta}(x)z^\beta$ defined by

$$\begin{aligned} -2i^n (zq)^{N+2} J_{(N,0)}(q^2) &\equiv \Pi_{(N)}^{\mu\nu;\alpha\beta}(q) (z^\nu z^\beta g^{\mu\alpha}) \\ &= \frac{\Pi_-(q^2) - \Pi_+(q^2)}{q^2} (qz)^2; \end{aligned} \quad (14)$$

the latter equality in (14) follows from (7) and (A.7) in Appendix A. This correlator contains the contributions from states with different parities, $\Pi_-(q^2)$ and $\Pi_+(q^2)$ (see the analysis in [4]); therefore, the contamination from the b_1 -meson ($J^{PC} = 1^{+-}$) in the phenomenological part of the corresponding SR is mandatory. The contamination makes it difficult to reliably extract the meson characteristics from this ‘‘mixed’’ SR.

The main feature of the theoretical part of $J_{(N,0)}(q^2)$ is the cancellation of the self-dual part, represented by the 4-quark condensate, in the anti-self-dual expression (14). The remaining ‘‘condensate’’ parts of (14) contain, after the Borel transformation, the same five universal elements $\Delta\Phi_\Gamma(x; M^2)$ as for the ρ^L - and the π -cases and, besides, an additional gluon contribution $\Delta\Phi'_G(x; M^2)$ (see Appendix B). This term affects the values of the moments rather strongly, as was shown in [8]. The contributions from the different kinds of NLC, $\Delta\Phi_\Gamma(x; M^2)$, are symbolically denoted in the r.h.s. of SR (15), so here we get rid of the 4-quark condensate which is not known very well due to a possible vacuum dominance violation. But the price we pay for this is a high sensitivity to the ill-known gluon contribution $\Delta\Phi'_G(x; M^2)$.

The method of calculation of the NLC contributions $\Delta\Phi_\Gamma(x; M^2)$ to the theoretical part of SR is described in [6–8]. The corrected final results of the calculation are presented in Appendix B which contains all the needed explicit expressions of $\Delta\Phi_\Gamma(x; M^2)$ for the simplest physically motivated Gaussian ansatz. The final SR including DAs of ρ -meson and the next resonances ρ' and b_1 into the phenomenological (left) part is as follows:

$$(f_\rho^{\text{T}})^2 \varphi_\rho^{\text{T}}(x) e^{-m_\rho^2/M^2}$$

$$\begin{aligned}
& +(\rho \rightarrow \rho') + (f_{b_1}^T)^2 \varphi_{b_1}^T(x) e^{-m_{b_1}^2/M^2} \\
& = \int_0^{s_b^T} \rho_T^{\text{mixed}}(x, s; s_\rho^T, s_b^T) e^{-s/M^2} ds \\
& \quad + \Delta\Phi_G(x; M^2) + \Delta\Phi'_G(x; M^2) \\
& \quad + \Delta\Phi_V(x; M^2) + \Delta\Phi_T(x; M^2), \tag{15}
\end{aligned}$$

where s_ρ^T and s_b^T are the effective continuum thresholds in the ρ - and b_1 -channels. Recall again that the variation of the ill-known part of the gluon contribution $\Delta\Phi'_G(x; M^2)$ can reduce the second moment significantly [8]. In the paper just mentioned, we suggest the following naive model: instead of the constant contribution $\Delta\varphi'_G(x; M^2) \equiv \langle \alpha_s GG \rangle / (6\pi M^2)$ (as in the standard approach), we put

$$\Delta\Phi'_G(x; M^2) = \Delta\varphi'_G(x; M^2) \frac{\theta(\Delta < x) \theta(x < 1 - \Delta)}{1 - 2\Delta}.$$

This simulation eliminates end-point ($x = 0, 1$) effects due to the influence of the vacuum gluon nonlocality; it is inspired by the analysis in [17] and our experience in the nonlocal quark case. The corresponding SR leads to the estimate $\langle \xi^2 \rangle_\rho^T = 0.329(11)$ (see Fig. 2a). However, this value drastically changes, $\langle \xi^2 \rangle_\rho^T \rightarrow 0.231(8)$, if we take the local expression $\Delta\varphi'_G(x; M^2)$ unchanged. Therefore, the estimate $\langle \xi^2 \rangle_\rho^T = 0.329$ contains a significant model uncertainty, and the actual value seems to be smaller.

Which prediction for this quantity can be obtained within the standard QCD SR approach? As one can see from Fig. 2b (long-dashed line), the value of $\langle \xi^2 \rangle_\rho^T$ cannot be estimated with a reasonable accuracy, because the standard SR *does not have real stability*. Nevertheless, the authors of [4] bravely deduce an estimate $\langle \xi^2 \rangle_\rho^T$ [B&B] = 0.27(4). We discuss this attempt in comparison with processing other SRs in greater detail in Sect. 5.

4 The “pure parity” sum rules

Using the approach of Sect. 2, we calculate OPE terms for the Π_\mp , $K_{1,3}$, and $K_{z,q}$ correlators and extract the contributions to DAs of the ρ - and b_1 -mesons. This allows us to write down the SRs for DAs of the ρ - and b_1 -mesons separately:

$$\begin{aligned}
& (m_\rho f_\rho^T)^2 \varphi_\rho^T(x) e^{-m_\rho^2/M^2} + (m_{\rho'} f_{\rho'}^T)^2 \varphi_{\rho'}^T(x) e^{-m_{\rho'}^2/M^2} \\
& = \frac{1}{2} \int_0^{s_\rho^T} \rho_T^{\text{pert}}(x; s) s e^{-s/M^2} ds \\
& \quad + \Delta\tilde{\Phi}_G(x; M^2) + \Delta\tilde{\Phi}_S(x; M^2) \\
& \quad + \Delta\tilde{\Phi}_V(x; M^2) + \Delta\tilde{\Phi}_T(x; M^2); \tag{16} \\
& (m_{b_1} f_{b_1}^T)^2 \varphi_{b_1}^T(x) e^{-m_{b_1}^2/M^2} \\
& = \frac{1}{2} \int_0^{s_b^T} \rho_T^{\text{pert}}(x; s) s e^{-s/M^2} ds \\
& \quad + \Delta\tilde{\Phi}_G(x; M^2) - \Delta\tilde{\Phi}_S(x; M^2) \\
& \quad + \Delta\tilde{\Phi}_V(x; M^2) + \Delta\tilde{\Phi}_T(x; M^2), \tag{17}
\end{aligned}$$

where $s_{\rho;b}^T$ are the effective continuum thresholds in the ρ - and the b_1 -meson cases, respectively. The perturbative spectral density $\rho_T^{\text{pert}}(x; s)$ is presented to the order of $O(\alpha_s)$ in [4, 8] (Appendix B). Here we also define the “tilded” functions

$$\Delta\tilde{\Phi}_\Gamma(x; M^2) \equiv \frac{1}{2} M^4 \partial_{M^2} \Delta\Phi_\Gamma(x; M^2), \tag{18}$$

and the whole tensor NLC contribution

$$\begin{aligned}
\Delta\tilde{\Phi}_T(x; M^2) & \equiv \Delta\tilde{\Phi}_{T_1}(x; M^2) + \Delta\tilde{\Phi}_{T_2}(x; M^2) \\
& \quad - \Delta\tilde{\Phi}_{T_3}(x; M^2). \tag{19}
\end{aligned}$$

The latter notably differs from the case of the longitudinally polarized ρ -meson due to the opposite sign of the T_3 -term, cf. [8]. The theoretical “condensate” part in (16) and (17) contains five elements obtained from (18) with the same $\Delta\tilde{\Phi}_\Gamma(x; M^2)$ as for the ρ^L -meson case, whereas the self-dual 4-quark contribution $\Delta\tilde{\Phi}_S(x; M^2)$ is a new element of the analysis. Note that just this self-dual part $\Delta\tilde{\Phi}_S(x; M^2)$, entering in the SRs (16) and (17) with different sign provides the different properties of the ρ - and b_1 -mesons [16].

For better understanding of the SR properties it is instructive to reduce them to the standard version for the $\langle \xi^N \rangle$ -moments. To this end, let us take the limits $\lambda_q^2 \rightarrow 0$, $\Delta\Phi_\Gamma(x; M^2) \rightarrow \Delta\varphi_\Gamma(x; M^2)$ in (16) and (17) and integrate over x with weights $(1 - 2x)^N$ to obtain the local limit version of the moment SR:

$$\begin{aligned}
& (m_\rho f_\rho^T)^2 \langle \xi^N \rangle_\rho^T e^{-m_\rho^2/M^2} \\
& = \frac{1}{2} \int_0^{s_\rho^T} \rho_T^{\text{pert}}(x; s) s e^{-s/M^2} ds - \frac{\langle \alpha_s GG \rangle}{24\pi} \left(\frac{N-1}{N+1} \right) \\
& \quad - \frac{16\pi \langle \sqrt{\alpha_s} \bar{q}(0) q(0) \rangle^2}{81 M^2} (4N-13). \tag{20}
\end{aligned}$$

This SR demonstrates a considerably lower sensitivity to the gluon condensate contribution: the gluon part does not depend on the Borel parameter M^2 at all, and its relative value is 6 times as low as that in the “mixed” SR. The r.h.s. of (20) is reduced at $N = 0$ to the known expression, see [4], that is not sensitive to the ρ' contribution, while its nonlocal version analyzed in [16] makes it possible to analyze the ρ' -meson. For $N > 0$, the SR is unstable due to the effect of radiative corrections, and to obtain the moment estimates we should return to the nonlocal version, (16).

But the price one pays for this is high: the fidelity windows of the SRs are significantly reduced. For the ρ -meson case, the fidelity windows of the Borel parameters M^2 shrink to $M^2 = 0.7\text{--}1.15 \text{ GeV}^2$ (to be compared with $M^2 = 0.75\text{--}2.25 \text{ GeV}^2$ in “mixed” SR) and demand one to take into account the ρ' -meson explicitly. Here we cannot obtain the ρ' -meson mass from SR (16) because of the enhanced perturbative spectral density ($\sim s$; this means that the differentiated SR has a spectral density $\sim s^2$ and presumably is not stable at all); instead, we use the ρ' -meson mass extracted in our previous paper

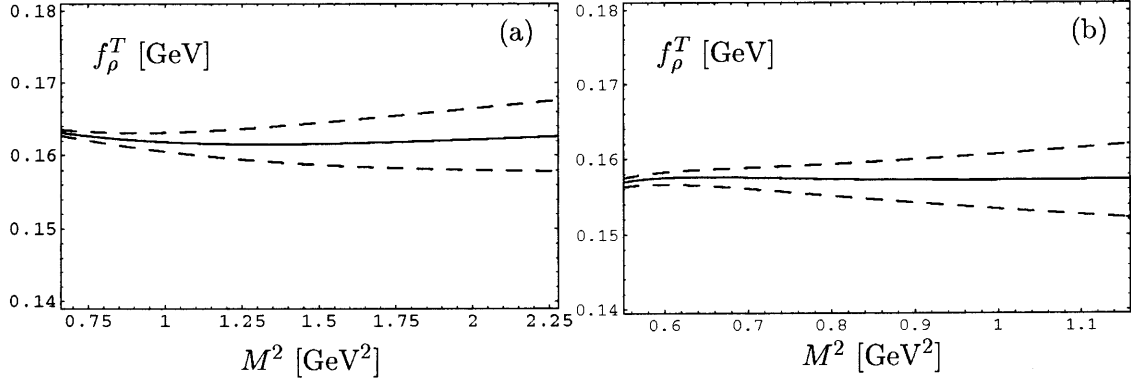


Fig. 1a,b. f_ρ^T as a function of the Borel parameter M^2 obtained from: **a** the “mixed parity” NLC SR, (15), with $s_0 = 2.9 \text{ GeV}^2$; **b** the “pure parity” NLC SR, (16), with $s_0 = 2.8 \text{ GeV}^2$. The fidelity windows for both figures coincide with the whole depicted range of M^2

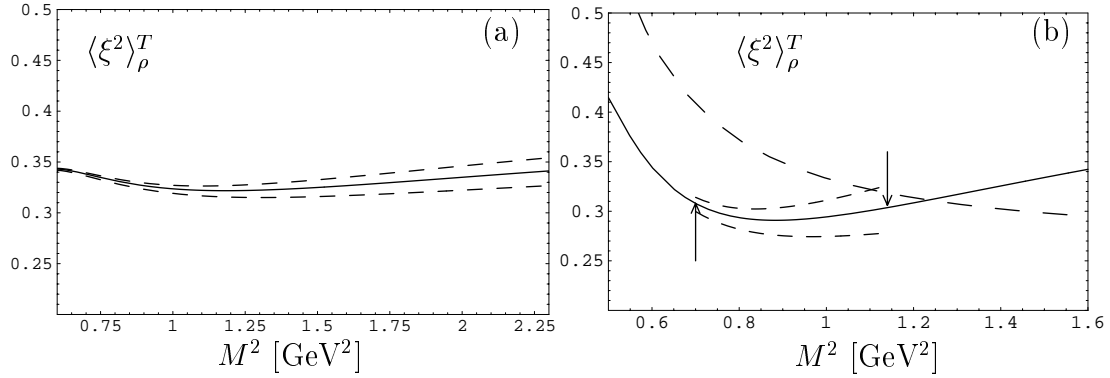


Fig. 2a,b. $\langle \xi^2 \rangle_\rho^T$ as a function of the Borel parameter M^2 obtained from: **a** the “mixed parity” NLC SR, (15), with $s_0 = 2.9 \text{ GeV}^2$; **b** the “pure parity” NLC SR, (16), with $s_0 = 2.8 \text{ GeV}^2$. Both kinds of SRs were processed taking the ρ' -meson into account; the arrows show the fidelity window (for **a** the window coincides with the whole depicted range of M^2). Solid lines correspond to the optimal thresholds s_0 , the short-dashed lines on both figures correspond to the curves with a 10%-variation of s_0 **a** or of χ_{\min}^2 **b**. The long-dashed line in **b** represents the SR of Ball–Braun [4]

on the longitudinally polarized ρ -meson DA [8], $m_{\rho'} = 1496 \pm 37 \text{ MeV}$, rather close to the Particle Data Group value $m_{\rho'} = 1465 \pm 22 \text{ MeV}$ [23].

In the case of the b_1 -meson, one can analyze only the SR for the zeroth moment (decay constant $f_{b_1}^T$) of the DA (see Fig. 3), the SRs for higher moments appearing to be invalid.

5 Processing different SRs and comparison of the results

We start with considering the results of processing both types of SRs for f_ρ^T . Its dependence on the Borel parameter M^2 obtained from the “mixed parity” NLC SR, (15), with $s_0 = 2.9 \text{ GeV}^2$ is shown in Fig. 1a. Figure 1b shows f_ρ^T as a function of the Borel parameter M^2 obtained from the “pure parity” NLC SR, (16), with $s_0 = 2.8 \text{ GeV}^2$. Both kinds of SRs are rather sensitive to the ρ' -meson contribution and, for this reason, they were processed taking it into account (see the numerical results in Table 1). Solid lines correspond to the optimal thresholds s_0 ; the dashed

lines to the curves with the 10-fold variation of χ_{\min}^2 (this corresponds approximately to a 5%-variation of s_0 ; for the definition of χ^2 see Appendix C, (C.1)). So one can conclude that both types of NLC SRs agree rather well on the value of f_ρ^T . Note that the presented f_ρ^T is rather close to the standard estimation $f_\rho^T = 0.160(10) \text{ GeV}$ [4] and to the lattice one, $f_{\rho_{\text{Latt}}}^T(4 \text{ GeV}^2) = 0.165(11) \text{ GeV}$ [24], and differs significantly from the result $f_\rho^T = 0.140 \text{ GeV}$ in [25].

Now we consider the results of processing SRs for the second moment $\langle \xi^2 \rangle_\rho^T$. First, we demonstrate the results of the “standard” approach: $\langle \xi^2 \rangle_\rho^T$ from (3.21) in [4] as a function of M^2 is shown in Fig. 2b by a long-dashed line. This curve is not stable in M^2 at all, therefore the SR can provide merely a range of admissible values, $0.27 \leq \langle \xi^2 \rangle_\rho^T \leq 0.4$. As is evident from Fig. 2, this wide window agrees reasonably with both the estimates from the “mixed” (a) and “pure” (b) NLC SRs.

Note that the authors of [4] dealt with the quantity a_2 , the Gegenbauer coefficient in the expansion of DA. The second moment of DA is trivially connected with this coefficient, $\langle \xi^2 \rangle = 0.2 + (12/35)a_2$. Using the SR of [4] for a_2 ,

Table 1. The estimate presented in this cell has been obtained by processing the “mixed parity” SR established in [4], whereas in the original paper [4] this value amounts to 0.27(4). The moments $\langle \xi^N \rangle_M(\mu^2)$ at $\mu^2 \sim 1 \text{ GeV}^2$ (errors are depicted in brackets in a standard manner)

Type of SR	$f_M(1 \text{ GeV}^2)$	$N = 2$	$N = 4$	$N = 6$	$N = 8$
Asympt. WF	1	0.2	0.086	0.047	0.030
NLC SR (16) : ρ^T	0.157(5)	0.296(20)	0.196(6)	0.132(5)	0.089(4)
NLC SR (15) : ρ^T	0.162(5)	0.329(11)	–	–	–
B&B SR : ρ^T	0.160(10)	0.304(40) ⁴	does not work		
NLC SR (16) : ρ^{T^T}	0.140(10)	0.086(6)	0.010(1)	0.013(1)	0.022(2)
NLC SR (17) : b_1^T	0.184(5)	does not work			
NLC SR (15) : b_1^T	0.181(5)	0.144(15)	–	–	–
B&B SR : b_1^T	0.175(5)	does not work			

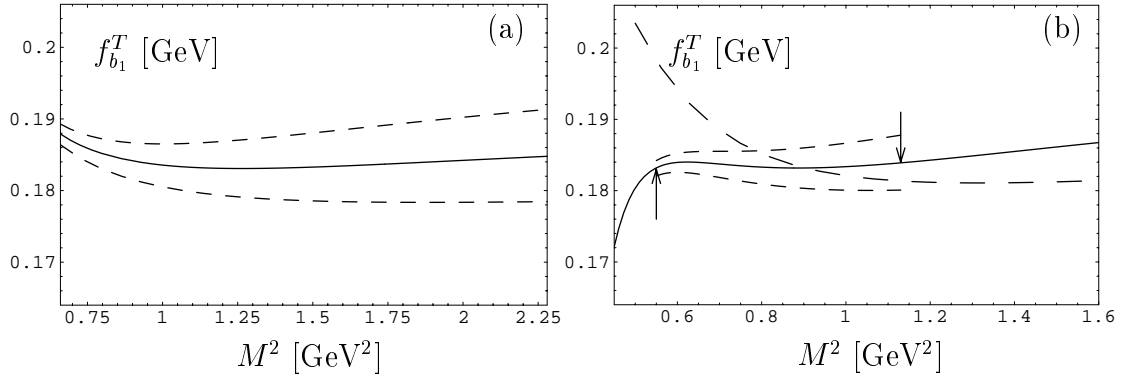


Fig. 3a,b. The curves $f_{b_1}^T$ in M^2 obtained from: **a** the “mixed parity” NLC SR (taking the ρ' -meson into account with $f_{\rho'}$ defined from “pure parity” SR (16)); **b** the “pure parity” NLC SR (17). The arrows show the fidelity window (for the right figure, the window coincides with the whole depicted range of M^2). Solid lines correspond to the optimal thresholds; the short-dashed lines on both figures to the curves with the 10-fold variation of χ_{\min}^2 ; the long-dashed line on the right figure corresponds to the real B&B curve

we obtain the corresponding window, $0.2 \leq a_2 \leq 0.4$, that leads to the mean value $\langle \xi^2 \rangle_{\rho[\text{Stand}]}^T = 0.30$ being surprisingly close to our estimate from NLC SRs (see Table 1). However, Ball and Braun have obtained the erroneous estimate $a_2 = 0.2 \pm 0.1$ producing, instead, the mean value $\langle \xi^2 \rangle_{\rho[\text{B\&B}]}^T = 0.27$.

The curves for the next higher moments, whose estimates are presented in Table 1, have fidelity windows and stability behavior similar to $\langle \xi^2 \rangle_{\rho}^T(M^2)$ in Fig. 2b. Finally, in Fig. 3, we demonstrate the very good correspondence between the values of $f_{b_1}^T$ obtained in different NLC SRs.

6 DA models and their check

Possible models of DAs corresponding to the moments in Table 1 are of the form

$$\varphi_{\rho}^{T,\text{mod}}(x, \mu^2) = 1.382 [\varphi^{as}(x)]^2$$

$$\begin{aligned} & \times \left(1 + 0.927 C_2^{3/2}(\xi) + 0.729 C_4^{3/2}(\xi) \right) \\ & = \varphi^{as}(x) \left(1 + 0.29 C_2^{3/2}(\xi) \right. \\ & \left. + 0.41 C_4^{3/2}(\xi) - 0.32 C_6^{3/2}(\xi) \right), \end{aligned} \quad (21)$$

$$\begin{aligned} \varphi_{\rho'}^{T,\text{mod}}(x, \mu^2) & = \varphi^{as}(x) \left(1 - 0.339 C_2^{3/2}(\xi) \right. \\ & \left. + 0.003 C_4^{3/2}(\xi) + 0.192 C_6^{3/2}(\xi) \right), \end{aligned} \quad (22)$$

$$\varphi_{b_1}^{\text{mod}}(x, \mu^2) = \varphi^{as}(x) \left(1 - (0.175 \pm 0.05) C_2^{3/2}(\xi) \right), \quad (23)$$

where $\xi \equiv 1 - 2x$, $C_n^{\nu}(\xi)$ are the Gegenbauer polynomials (GP), and the norm $\mu^2 \simeq 1 \text{ GeV}^2$ corresponds to a mean value of M^2 . Recall again that the value of the important coefficient $a_2 = 0.29$ in (21) is confirmed by three sources: “pure” NLC SR (16), “mixed” NLC SR (15), and a mean value from the “mixed” standard SR. Figures 4 and 5a contain curves of DA corresponding to ρ_{\perp} , (21), and ρ'_{\perp} (22). The arising 3-hump shape of DA for ρ_{\perp} dras-

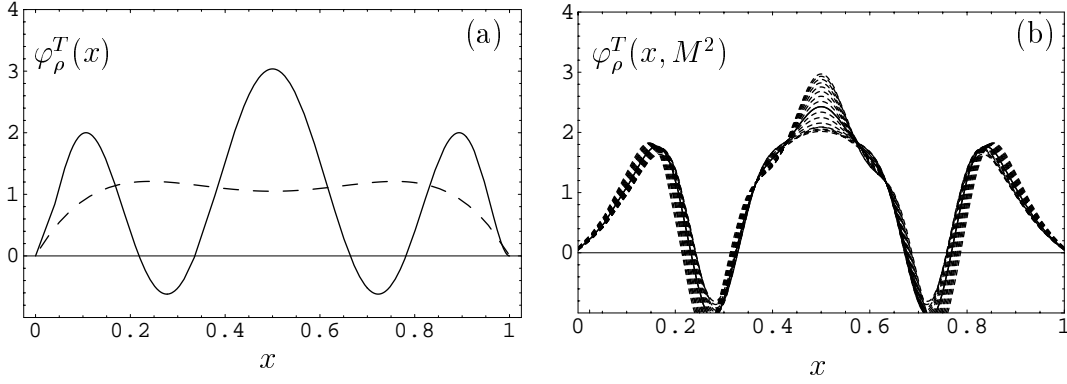


Fig. 4. **a** The curves of $\varphi_\rho^{\text{T,mod}}(x, 1 \text{ GeV}^2)$: Solid lines correspond to the best fits for the moments determined (see Table 1); the dashed line on the left figure corresponds to the B&B curve (which fits only $\langle \xi^2 \rangle_\rho^{\text{T}} \approx 0.27$). **b** The r.h.s. of (16) $\text{SR}_\rho^{\text{T}}(x, M^2)$ in x . Different lines here correspond to different values of the Borel parameter $M^2 = 0.7\text{--}0.9 \text{ GeV}^2$

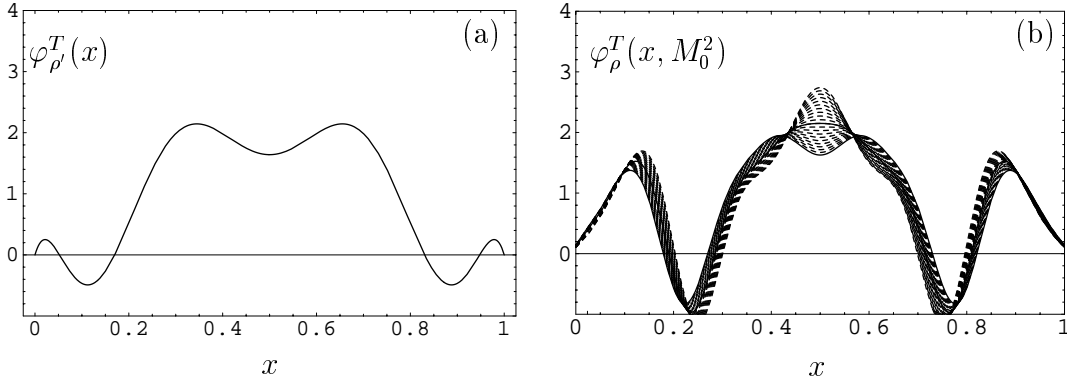


Fig. 5. **a** The curve of $\varphi_{\rho'}^{\text{T,mod}}(x, 1 \text{ GeV}^2)$ as a function of x . **b** The r.h.s. of (16) $\text{SR}_{\rho'}^{\text{T}}(x, M_0^2)$ as a function of x . Solid and dashed lines here correspond to different values of the nonlocality parameter $\lambda_q^2 = 0.4\text{--}0.5 \text{ GeV}^2$ with fixed value of the Borel parameter $M_0^2 = 0.8 \text{ GeV}^2$

tically differs from the one obtained in [4] and from the one obtained in chiral effective theory [25].

This difference mainly appears due to the higher moments, $N = 4, 6, 8$, involved in the consideration. Nevertheless, the hump shape is not an artifact of the GP expansion series truncation. These models really contain only three first GPs; meanwhile, it is enough to reproduce all four moments up to $N = 8$. Moreover, an additionally smoothed⁵ r.h.s. of the NLC SR (16) qualitatively demonstrates the same behavior in x (at admissible M^2) as the model DA; compare Figs. 4a,b. The stability of the DA shape with respect to the variation of ansatz is also checked. To this end, we show in Fig. 5b the same r.h.s. of (16) as in Fig. 4b, but with different values of the single ansatz parameter $\lambda_q^2 = 0.4\text{--}0.5 \text{ GeV}^2$ at the fixed value $M_0^2 = 0.8 \text{ GeV}^2$.

Inverse moments of DAs often appear in perturbative QCD predictions for exclusive reactions. The estimates for important $\langle x^{-1} \rangle_M$ moments obtained from the model DAs are presented here⁶:

⁵ A certain smoothing of some δ -functions in the r.h.s. of the SR (see Appendix B) is not important

⁶ The upper error $+0.4$ in (24) corresponds to an overestimate $\langle \xi^2 \rangle = 0.329$ from the “mixed” SR

$$\begin{aligned} \langle x^{-1} \rangle_\rho &\equiv \int_0^1 \frac{\varphi_\rho^{\text{T}}(x, 1 \text{ GeV}^2)}{x} dx \\ &= \begin{cases} 4.15_{-0.1}^{+0.4} & (\text{here}), \\ 3.6 & (\text{B\&B model}), \end{cases} \end{aligned} \quad (24)$$

$$\begin{aligned} \langle x^{-1} \rangle_{\rho'} &\equiv \int_0^1 \frac{\varphi_{\rho'}^{\text{T}}(x, 1 \text{ GeV}^2)}{x} dx = 2.57 \pm 0.20 \\ &(\text{here}), \end{aligned} \quad (25)$$

$$\begin{aligned} \langle x^{-1} \rangle_{b_1} &\equiv \int_0^1 \frac{\varphi_{b_1}^{\text{T}}(x, 1 \text{ GeV}^2)}{x} dx = 2.48 \pm 0.20 \\ &(\text{here}). \end{aligned} \quad (26)$$

It is useful to construct an *independent* SR for these inverse moments to verify the DA models (21), (22) and (23). Namely, the weighted sum $C(M^2)$ of these moments,

$$\begin{aligned} C(M^2) &\equiv \langle x^{-1} \rangle_\rho + \langle x^{-1} \rangle_{\rho'} \left(\frac{f_{\rho'}^{\text{T}}}{f_\rho^{\text{T}}} \right)^2 e^{-(m_{\rho'}^2 - m_\rho^2)/M^2} \\ &+ \langle x^{-1} \rangle_{b_1} \left(\frac{f_{b_1}^{\text{T}}}{f_\rho^{\text{T}}} \right)^2 e^{-(m_{b_1}^2 - m_\rho^2)/M^2}, \end{aligned} \quad (27)$$

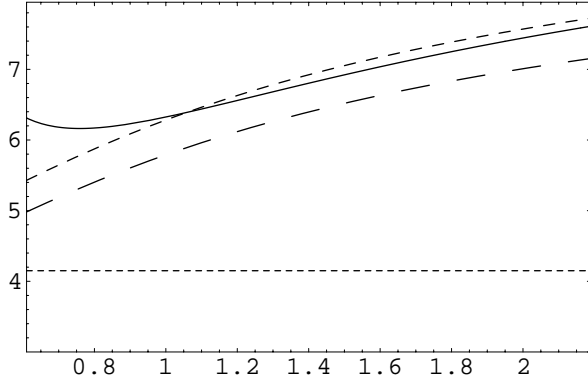


Fig. 6. $C(M^2)$ as a function of M^2 (solid line) determined by (27) and integrating over x (15) in comparison with the l.h.s. of (28) (long-dashed line). The dotted line corresponds to $\langle x^{-1} \rangle_\rho = 4.15$; whereas the dashed line corresponds to the l.h.s. of (28) with upper values of corresponding moments

can be obtained by integrating the r.h.s. of the “mixed” NLC SR (15) with the weight $1/x$. A comparison of the function $C(M^2)$ with the corresponding combination of model estimates (24), (25) and (26) obtained in different kinds of NLC SRs (mainly from the “pure” ones) leads to the approximate equation

$$\begin{aligned} & 4.15 + 2.57 \left(\frac{f_{\rho'}^T}{f_\rho^T} \right)^2 e^{-(m_{\rho'}^2 - m_\rho^2)/M^2} \\ & + 2.48 \left(\frac{f_{b_1}^T}{f_\rho^T} \right)^2 e^{-(m_{b_1}^2 - m_\rho^2)/M^2} \\ & \approx C(M^2), \end{aligned} \quad (28)$$

illustrated in Fig. 6.

As a result, one can conclude to the following.

- (1) The “mixed” NLC SR is highly sensitive to b_1 - and ρ' -meson contributions; the difference in the behavior of $C(M^2)$ (solid line) and in the ρ -contribution alone (dotted line) illustrates this point.
- (2) The curve $C(M^2)$ lies between the mean and upper estimates for the l.h.s. of (28), so it is in reasonable agreement with the estimates (24), (25) and (26). It also demonstrates an overestimation of the DA moments in the “mixed” SR as compared to that obtained from the “pure” one.

7 DA models and the $B \rightarrow \rho e \nu$ decay form factors

The new DA shapes result in different pQCD predictions for exclusive reactions with the ρ -meson. As an example, we re-estimate the form factors $V(t)$, $A_{1,2}(t)$ corresponding to the transition matrix element $\langle \rho, \lambda | (V - A)_\mu | B \rangle$ of the process $B \rightarrow \rho e \nu$, in the framework of the light-cone SR approach [26]. That was done earlier by Ball and Braun in [27, 28] on the base of DAs from [4]. Thus, to estimate the influence of the new nonperturbative input presented

in the previous sections, we have used the LC SR in the leading twist approximation (cf. [27]). Just as in the case of the LC expansion for the transition amplitude $\gamma^* \gamma \rightarrow \pi^0$, one might expect a high sensitivity to the end-point behavior of the DAs, as they enter into convolution integrals like $\langle x^{-1} \rangle_M$ estimated in (24).

However, there are some essential differences which effectively soften our expectations. First, the DAs also enter into the “phenomenological” side of the SR in the “continuum” contribution of higher excited states in the channel with B -meson quantum numbers. This, actually, is a specific feature of any LC SR. By subtracting the “continuum”, one actually obtains “infrared safe quantities” like $\int_\epsilon^1 dx \varphi(x)/x$ where $\epsilon \simeq (m_b^2 - t)/(s_0^B - t)$, $m_b \simeq 4.8 \text{ GeV}$, and $s_0^B \simeq 34 \text{ GeV}^2$ is the continuum threshold in the B -channel⁷ as defined from the 2-point QCD SRs for the B -meson decay constant f_B (see [29]). For $t \approx 0$, $\epsilon \simeq 0.5\text{--}0.6$ and the LC SR should not be so sensitive to the end-point region $x \sim 0$. Obviously, the end-point region becomes important for higher momentum transfers t . However, for $t \geq 20 \text{ GeV}^2$ the LC expansion would hardly make sense. The second factor which eventually decreases the importance of the end-point region is connected with the standard Borel transformation of the SR with respect to the virtuality of the B -meson current: $-p_B^2 \rightarrow M_B^2$. The corresponding contribution from the coefficient function produces a standard suppression exponent: $\exp(\bar{x}(t - m_b^2)/xM_B^2)$. Numerically, it turned out to be less important.

We have treated the LC SRs using the same input parameters and the same procedure of extracting the physical form factors as in [27]. However, if one tries to fix the onset of the “continuum” by hand to the value $s_0^B \simeq 34 \text{ GeV}^2$ dictated by the 2-point SRs for f_B , one encounters *inadmissible* uncertainties in the determination of the form factors when using our new nonperturbative input DAs. To get a stable SR, one is forced to allow a higher value for the s_0^B parameter.

Below, the form factor values are written at a zero momentum transfer ($t = 0$) as compared with B&B results:

$$\begin{aligned} V(0) &= \begin{cases} 0.37(1) \text{ (here } [s_0 = 50 \text{ GeV}^2], \chi^2 \approx 0.4), \\ 0.35(2) \text{ ([27] } [s_0 = 34 \text{ GeV}^2], \chi^2 \approx 3.4), \end{cases} \\ A_1(0) &= \begin{cases} 0.283(4) \text{ (here } [s_0 = 45 \text{ GeV}^2], \chi^2 \approx 0.1), \\ 0.27(1) \text{ ([27] } [s_0 = 34 \text{ GeV}^2], \chi^2 \approx 1.1), \end{cases} \\ A_2(0) &= \begin{cases} 0.30(1) \text{ (here } [s_0 = 50 \text{ GeV}^2], \chi^2 \approx 0.2), \\ 0.28(1) \text{ ([27] } [s_0 = 34 \text{ GeV}^2], \chi^2 \approx 1.1). \end{cases} \end{aligned} \quad (29)$$

Our form factors are slightly higher than those in [27] and possess a better accuracy (compare χ^2 in (29)). The difference becomes more pronounced for a large value of the momentum transfer t , ($m_b^2 - t \sim \mathcal{O}(m_b)$). This is not surprising due to the higher sensitivity to the end-point behavior of the input DA in this region. The form factors presented are determined with new “optimal” thresholds s_0^B providing a few times better processing accuracy. Note

⁷ As we shall see below, the LC SRs “prefer” a higher value

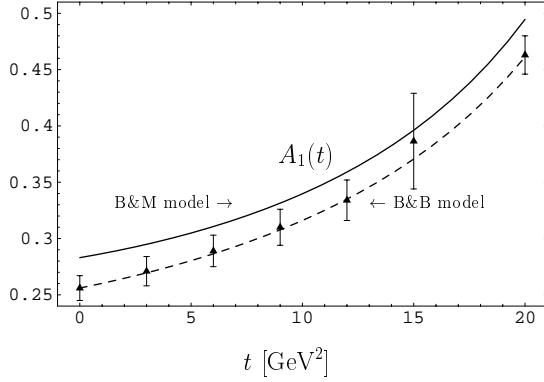


Fig. 7. Form factor $A_1(t)$; the solid line corresponds to our processing of LC QCD SR, the dashed line to processing following the B&B formulas ([27]) (the bars in the figure show the errors of the B&B calculations)

that the parameters of the usual “pole” parameterization of the form factors change significantly as compared to that in [27], e.g.,

$$A_1(t) = \frac{0.283}{1 - 0.157(t/m_B^2) - 0.837(t/m_B^2)^2}$$

The important form factor $A_1(t)$ (solid line) increases about 5–10% in comparison with the B&B result (the bars in the figure show the errors of the B&B calculations), with an optimal threshold $s_0^B \simeq 45 \text{ GeV}^2$.

8 Conclusion

Let us summarize the main results of this paper.

(1) We construct NLC SRs for DA for each P -parity channel, based on the properties of the duality transformation. The negative parity NLC SR for transversely polarized ρ -, ρ' -mesons works rather well and allows us to estimate the 2nd, 4th, 6th, and 8th moments of the leading twist DAs. The positive parity SR for the transversely polarized b_1 -meson can provide only the value of the b_1 -meson lepton decay constant, $f_{b_1}^T$. It should be emphasized that an analogous evaluation of the moments within the standard QCD SR approach is impossible.

(2) Results of processing different NLC SRs of the “pure” (see Figs. 1b, 2b, 3b) and “mixed” (see Figs. 1a, 2a, 3a) parity are compared, and a reasonable agreement is found. The “mixed” SR in the standard version admits merely a window of possible values of the second moment $\langle \xi^2 \rangle$ (see, e.g., [4]); the position of the window is corrected here and, as a result, agrees with the NLC SR results presented in Table 1.

(3) The models for the leading twist DAs of the ρ_\perp - and ρ'_\perp -mesons, (21) and (22), and of the b_1^- -meson, (23), are suggested. The shape of a new ρ_\perp -meson distribution (see Fig. 4a) drastically differs from that obtained by Ball and Braun [4] only on the basis of the value $a_2 = 0.2$. The latter estimate is discussed in Sect. 5.

(4) We estimate important integrals appearing in perturbative QCD predictions for different exclusive reactions,

$$\langle x^{-1} \rangle_M \equiv \int_0^1 \frac{\varphi_M^T(x)}{x} dx$$

in (24)–(26), based on our results for the DA shapes. We check the self-consistency of these results by comparing them with those obtained from an independent “mixed” QCD SR for the inverse moment $\langle x^{-1} \rangle_M$ and find agreement.

(5) Form factors of the process $B \rightarrow \rho e \nu$, $V(t)$, $A_{1,2}(t)$, where t is the momentum transfer, are also re-estimated in the framework of the light-cone SR approach [27] on the basis of the new model for the ρ -meson DAs; the results are slightly higher and have uncertainties a few times smaller than those obtained by Ball and Braun.

Finally, we can conclude that the nonlocal condensate QCD SR approach to the distribution amplitudes is self-consistent and gives reliable results. An open problem of this approach is to determine well-established models of the distribution functions $f_T(\nu)$ from the theory of the nonperturbative QCD vacuum. First direct attempts to calculate quark NLC have been done in lattice simulations in [21]. The “short distance” correlation length of NLC has also been extracted later in [22]; it turns out to be reasonably close to the value of $1/\lambda_q$ and confirms the validity of our Gaussian NLC model.

Acknowledgements. This work was partially supported by the Russian Foundation for Basic Research (grant N 00-02-16696) and Heisenberg–Landau Program. We are grateful to R. Ruskov for help in a better understanding of B decay (Sect. 8), to O.V. Teryaev, M. Polyakov, and N.G. Stefanis for fruitful discussions. We gratefully acknowledge the warm hospitality of Prof. K. Goetze and Dr. Dr. N.G. Stefanis at Bochum University, where this work was completed.

A Decomposition of rank-4 tensor $\Pi_{(N)}^{\mu\nu;\alpha\beta}$

Now follow expressions that are made use of in this article:

$$P_1^{\mu\nu;\alpha\beta} \equiv \frac{1}{2q^2} [g^{\mu\alpha} q^\nu q^\beta - g^{\nu\alpha} q^\mu q^\beta - g^{\mu\beta} q^\nu q^\alpha + g^{\nu\beta} q^\mu q^\alpha], \quad (\text{A.1})$$

$$P_2^{\mu\nu;\alpha\beta} \equiv \frac{1}{2} [g^{\mu\alpha} g^{\nu\beta} - g^{\mu\beta} g^{\nu\alpha}] - P_1^{\mu\nu;\alpha\beta}, \quad (\text{A.2})$$

$$Q_1^{\mu\nu;\alpha\beta} \equiv \frac{1}{2(qz)} [g^{\mu\alpha} q^\nu z^\beta + g^{\nu\beta} q^\mu z^\alpha - g^{\mu\beta} q^\nu z^\alpha - g^{\nu\alpha} q^\mu z^\beta], \quad (\text{A.3})$$

$$Q_3^{\mu\nu;\alpha\beta} \equiv \frac{1}{2(qz)} [g^{\mu\alpha} z^\nu q^\beta + g^{\nu\beta} z^\mu q^\alpha - g^{\mu\beta} z^\nu q^\alpha - g^{\nu\alpha} z^\mu q^\beta], \quad (\text{A.4})$$

$$Q_z^{\mu\nu;\alpha\beta} \equiv \frac{q^2}{2(qz)^2} [g^{\mu\alpha} z^\nu z^\beta + g^{\nu\beta} z^\mu z^\alpha - g^{\mu\beta} z^\nu z^\alpha - g^{\nu\alpha} z^\mu z^\beta], \quad (\text{A.5})$$

$$Q_q^{\mu\nu;\alpha\beta} \equiv \frac{1}{2(qz)^2} (q^\alpha z^\beta - q^\beta z^\alpha) (q^\mu z^\nu - q^\nu z^\mu). \quad (\text{A.6})$$

$$g^{\mu\alpha} z^\nu z^\beta P_1^{\mu\nu;\alpha\beta} \equiv P_1^{\mu z;\mu z} = -P_2^{\mu z;\mu z} = \frac{(qz)^2}{q^2},$$

$$Q_1^{\mu z;\mu z} = Q_3^{\mu z;\mu z} = Q_z^{\mu z;\mu z} = Q_q^{\mu z;\mu z} = 0, \quad (\text{A.7})$$

$$q^\mu q^\alpha z^\nu z^\beta P_1^{\mu\nu;\alpha\beta} \equiv P_1^{qz;qz} = Q_1^{qz;qz} = Q_3^{qz;qz} = -Q_q^{qz;qz}$$

$$= -\frac{(qz)^2}{2},$$

$$P_2^{qz;qz} = Q_z^{qz;qz} = 0. \quad (\text{A.8})$$

Let us write down the parameterization of matrix elements of a composite tensor current operator, see, e.g., [28]:

$$\langle 0 | \bar{d}(z) \sigma_{\mu\nu} u(0) | \rho_\perp(p, \lambda) \rangle \Big|_{z^2=0}$$

$$= i f_{\rho_\perp}^T \left[(\varepsilon_\mu(p, \lambda) p_\nu - \varepsilon_\nu(p, \lambda) p_\mu) \int_0^1 dx \varphi_\rho^T(x) e^{ix(zp)} \right.$$

$$+ (\varepsilon_\mu(p, \lambda) z_\nu - \varepsilon_\nu(p, \lambda) z_\mu) p^2 \int_0^1 dx V_1(x) e^{ix(zp)}$$

$$\left. + (p^\mu z_\nu - p^\nu z_\mu) (\varepsilon(p, \lambda) z) p^2 \int_0^1 dx V_2(x) e^{ix(zp)} \right], \quad (\text{A.9})$$

$$\langle 0 | \bar{d}(z) \sigma_{\mu\nu} u(0) | b_1(p, \lambda) \rangle \Big|_{z^2=0}$$

$$= f_{b_1}^T \left[\varepsilon_{\mu\nu\alpha\beta} \varepsilon^\alpha(p, \lambda) p^\beta \int_0^1 dx \varphi_{b_1}(x) e^{ix(zp)} \right.$$

$$+ \varepsilon_{\mu\nu\alpha\beta} \varepsilon^\alpha(p, \lambda) z^\beta p^2 \int_0^1 dx U_1(x) e^{ix(zp)}$$

$$\left. + \varepsilon_{\mu\nu\alpha\beta} p^\alpha z^\beta (\varepsilon(p, \lambda) z) p^2 \int_0^1 dx U_2(x) e^{ix(zp)} \right]. \quad (\text{A.10})$$

Here we decode our shorthand notation used in Sect. 2:

$$v_0 \equiv |f_{\rho_\perp}^T|^2 \langle x^N \rangle_{\rho_\perp}, \quad v_1 \equiv |f_{\rho_\perp}^T|^2 \langle -iN x^{N-1} \rangle_{V_1},$$

$$v_2 \equiv |f_{\rho_\perp}^T|^2 \langle -N(N-1) x^{N-2} \rangle_{V_2}, \quad u_0 \equiv |f_{b_\perp}^T|^2 \langle x^N \rangle_{b_\perp},$$

$$u_1 \equiv |f_{b_\perp}^T|^2 \langle -iN x^{N-1} \rangle_{U_1},$$

$$u_2 \equiv |f_{b_\perp}^T|^2 \langle -N(N-1) x^{N-2} \rangle_{U_2}$$

(with $\langle f(x) \rangle_U \equiv \int_0^1 dx f(x) U(x)$). In the general case, the whole system of equations for different twist DA contributions is of the following form:

$$\frac{\Pi_-(q^2, qz)}{2(qz)^N q^2} = -v_0 + u_1 + u_2, \quad \frac{K_1(q^2, qz)}{2(qz)^N q^2} = -v_1 - u_2,$$

$$\frac{K_z(q^2, qz)}{2(qz)^N q^2} = +u_2, \quad (\text{A.11})$$

$$\frac{\Pi_+(q^2, qz)}{2(qz)^N q^2} = +u_0 + u_1 + u_2, \quad \frac{K_3(q^2, qz)}{2(qz)^N q^2} = -u_1 - u_2,$$

$$\frac{K_q(q^2, qz)}{2(qz)^N q^2} = v_2 - u_2. \quad (\text{A.12})$$

B Expressions for nonlocal contributions to SR

To construct SR for distribution amplitudes, it is useful to parameterize NLC behaviors by the ‘‘distribution functions’’ [7, 8, 13, 14] à la α -representation of the propagators, e.g., $f_S(\alpha)$ for the scalar condensate $M_S(z^2)$ ⁸:

$$M_S(z^2) = \langle \bar{q}(0) q(0) \rangle \int_0^\infty e^{\alpha z^2/4} f_S(\alpha) d\alpha,$$

where

$$\int_0^\infty f_S(\alpha) d\alpha = 1, \quad \int_0^\infty \alpha f_S(\alpha) d\alpha = \frac{\lambda_q^2}{2}, \quad (\text{B.1})$$

and for the vector condensate $M_V^\mu(z^2)$,

$$M_V^\mu(z) \equiv \langle \bar{q}(0) \gamma^\mu q(z) \rangle = -iz^\mu \frac{A_S}{4} \int_0^\infty e^{\alpha z^2/4} f_V(\alpha) d\alpha,$$

where

$$\int_0^\infty f_V(\alpha) d\alpha = 0. \quad (\text{B.2})$$

Here and in the following we take quark and gluon fields in the fixed point gauge, $z^\mu A_\mu(z) = 0$, where the path-ordered exponential $E(0, z) = 1$. The $M_{\mu\nu}$ ($\tilde{M}_{\mu\nu}$) appearing in the SR quark–gluon–quark NLC,

$$M_{\mu\nu}(y, z) \equiv \langle \bar{q}(0) \gamma_\nu \hat{A}_\mu(z) q(y) \rangle$$

$$= (y_\mu z_\nu - g_{\mu\nu}(zy)) \cdot M_{T1}$$

$$+ (z_\mu z_\nu - g_{\mu\nu} z^2) \cdot M_{T2} + \dots, \quad (\text{B.3})$$

$$\tilde{M}_{\mu\nu}(y, z) \equiv \langle \bar{q}(0) \gamma_\nu (\gamma_5) \hat{A}_\mu(z) q(y) \rangle$$

$$= \varepsilon_{\mu\nu\rho\sigma} z_\rho y_\sigma \cdot M_{T3} + \dots, \quad (\text{B.4})$$

can be decomposed in form factors M_{T1-T3} , where the tensors in front of them satisfy the gauge condition $z^\mu M_{\mu\nu}$ ($\tilde{M}_{\mu\nu}$) = 0 (since $z^\mu \hat{A}_\mu(z) = 0$). The NLC M_{T1-T3} can be parameterized by a triple integral representation:

$$M_{Ti}(z^2, y^2, (z-y)^2)$$

$$= A_{Ti} \int_0^\infty e^{(\alpha_1 z^2/4 + \alpha_2 y^2/4 + \alpha_3 (z-y)^2/4)}$$

$$\times f_i(\alpha_1, \alpha_2, \alpha_3) d\alpha_1 d\alpha_2 d\alpha_3, \quad (\text{B.5})$$

where

$$A_{Ti} = \left\{ -\frac{3}{8} A_S, \frac{1}{2} A_S, \frac{3}{8} A_S \right\},$$

⁸ In deriving these sum rules we can always make a Wick rotation, i.e., we assume that all coordinates are Euclidean, $z^2 < 0$

and

$$A_S = \frac{8\pi}{81} \langle \sqrt{\alpha_s} \bar{q}(0)q(0) \rangle^2.$$

The function $f_S(\alpha)$ and other similar functions $f_\Gamma(\alpha)$ describe distributions of vacuum fields in virtuality α for every type (Γ) of NLC. The convolutions $\Delta\Phi_\Gamma(x, M^2)$ of the distribution functions f_Γ and coefficient functions completely determine the r.h.s. of the SRs, so $\Delta\Phi_\Gamma$ depends on the model of the f_Γ . For the vacuum distribution functions $f_\Gamma(\alpha)$, we use the set of the simplest ansatzes

$$\begin{aligned} f_S(\alpha) &= \delta(\alpha - \lambda_q^2/2), \\ f_V(\alpha) &= \delta'(\alpha - \lambda_q^2/2), \end{aligned} \quad (\text{B.6})$$

$$\begin{aligned} f_{T_{1,2,3}}(\alpha_1, \alpha_2, \alpha_3) &= \delta(\alpha_1 - \lambda_q^2/2) \delta(\alpha_2 - \lambda_q^2/2) \\ &\times \delta(\alpha_3 - \lambda_q^2/2). \end{aligned} \quad (\text{B.7})$$

Their meaning and relation to the initial NLCs have been discussed in detail in [6, 7]. The contributions $\Delta\Phi_\Gamma(x, M^2)$ to the r.h.s. of SR, corresponding to these ansatzes, are shown below. The limit of these expressions to the standard (local) contributions $\varphi_\Gamma(x, M^2)$, $\lambda_q^2 \rightarrow 0$, $\Delta\Phi_\Gamma(x, M^2) \rightarrow \Delta\varphi_\Gamma(x, M^2)$ are also written for comparison. Hereafter $\Delta \equiv \lambda_q^2/(2M^2)$, $\bar{\Delta} \equiv 1 - \Delta$:

$$\begin{aligned} \Delta\Phi_S(x, M^2) &= \frac{A_S}{M^4} \frac{18}{\Delta\bar{\Delta}^2} \\ &\times \{ \theta(\bar{x} > \Delta > x) \bar{x} [x + (\Delta - x) \ln(\bar{x})] + (\bar{x} \rightarrow x) \\ &+ \theta(1 > \Delta) \theta(\Delta > x > \bar{\Delta}) [\bar{\Delta} + (\Delta - 2\bar{x}x) \ln(\Delta)] \}, \end{aligned} \quad (\text{B.8})$$

$$\begin{aligned} \Delta\varphi_S(x, M^2) &= \frac{A_S}{M^4} 9(\delta(x) + (\bar{x} \rightarrow x)), \\ \Delta\Phi_V(x, M^2) &= \frac{A_S}{M^4} (x\delta'(\bar{x} - \Delta) + (\bar{x} \rightarrow x)), \end{aligned} \quad (\text{B.9})$$

$$\Delta\varphi_V(x, M^2) = \frac{A_S}{M^4} (x\delta'(\bar{x}) + (\bar{x} \rightarrow x)),$$

$$\begin{aligned} \Delta\Phi_{T_1}(x, M^2) &= -\frac{3A_S}{M^4} \theta(1 > 2\Delta) \left\{ [\delta(x - 2\Delta) - \delta(x - \Delta)] \left(\frac{1}{\Delta} - 2 \right) \right. \\ &+ \theta(2\Delta > x) \cdot \theta(x > \Delta) \frac{\bar{x}}{\Delta} \left[\frac{x - 2\Delta}{\Delta\bar{\Delta}} \right] \left. \right\} \\ &+ (\bar{x} \rightarrow x), \end{aligned} \quad (\text{B.10})$$

$$\begin{aligned} \Delta\varphi_{T_1}(x, M^2) &= \frac{3A_S}{M^4} (\delta'(\bar{x}) + (\bar{x} \rightarrow x)), \\ \Delta\Phi_{T_2}(x, M^2) &= \frac{4A_S}{M^4} \bar{x} \theta(1 > 2\Delta) \\ &\times \left\{ \frac{\delta(x - 2\Delta)}{\Delta} - \theta(2\Delta > x) \theta(x > \Delta) \right. \\ &\times \left. \frac{1 + 2x - 4\Delta}{\Delta\bar{\Delta}^2} \right\} + (\bar{x} \rightarrow x), \end{aligned} \quad (\text{B.11})$$

$$\begin{aligned} \Delta\varphi_{T_2}(x, M^2) &= -\frac{2A_S}{M^4} (x\delta'(\bar{x}) + (\bar{x} \rightarrow x)), \\ \Delta\Phi_{T_3}(x, M^2) &= \frac{3A_S\bar{x}}{M^4\bar{\Delta}\Delta} \\ &\times \{ \theta(2\Delta > x) \theta(x > \Delta) \theta(1 > 2\Delta) \\ &\times \left[2 - \frac{\bar{x}}{\Delta} - \frac{\Delta}{\bar{\Delta}} \right] \} + (\bar{x} \rightarrow x), \end{aligned} \quad (\text{B.12})$$

$$\begin{aligned} \Delta\varphi_{T_3}(x, M^2) &= \frac{3A_S}{M^4} (\delta(\bar{x}) + (\bar{x} \rightarrow x)), \\ \Delta\Phi_G(x, M^2) &= \frac{\langle \alpha_s GG \rangle}{24\pi M^2} (\delta(x - \Delta) + (\bar{x} \rightarrow x)), \end{aligned} \quad (\text{B.13})$$

$$\begin{aligned} \Delta\varphi_G(x, M^2) &= \frac{\langle \alpha_s GG \rangle}{24\pi M^2} (\delta(\bar{x}) + (\bar{x} \rightarrow x)), \\ \Delta\Phi'_G(x, M^2) &= \frac{\langle \alpha_s GG \rangle}{6\pi M^2} \\ &\times \frac{\theta(\Delta < x) \theta(x < 1 - \Delta)}{1 - 2\Delta}, \end{aligned} \quad (\text{B.14})$$

$$\Delta\varphi'_G(x, M^2) = \frac{\langle \alpha_s GG \rangle}{6\pi M^2}.$$

For quark and gluon condensates, we use the standard estimates [30]

$$\begin{aligned} \langle \sqrt{\alpha_s} \bar{q}(0)q(0) \rangle &\approx (-0.238 \text{ GeV})^3, \\ \frac{\langle \alpha_s GG \rangle}{12\pi} &\approx 0.001 \text{ GeV}^4 \end{aligned}$$

and

$$\lambda_q^2 = \frac{\langle \bar{q}(ig\sigma_{\mu\nu}G^{\mu\nu})q \rangle}{2\langle \bar{q}q \rangle} = 0.4 \div 0.5 \text{ GeV}^2$$

normalized at $\mu^2 \approx 1 \text{ GeV}^2$.

As regards expressions for the perturbative spectral density, we have radiative corrections reach 10% of the Born result at $s \sim 1 \text{ GeV}^2$. Now

$$\begin{aligned} \rho_T^{\text{pert}}(x, s) &= \frac{3}{2\pi^2} x\bar{x} \left\{ 1 + \frac{\alpha_s(\mu^2)C_F}{4\pi} \left(2\ln \left[\frac{s}{\mu^2} \right] + 6 \right. \right. \\ &\left. \left. - \frac{\pi^2}{3} + \ln^2(\bar{x}/x) + \ln(x\bar{x}) \right) \right\}. \end{aligned} \quad (\text{B.15})$$

Here $\mu^2 \sim 1 \text{ GeV}^2$ corresponds to the average value of the Borel parameter M^2 in the stability window; $\alpha_s(1 \text{ GeV}^2) \approx 0.52$. We also use the ‘‘mixed’’ perturbative spectral density suggested in [31] in the ‘‘mixed’’ SR:

$$\begin{aligned} \rho_T^{\text{mixed}}(x, s; s_\rho^T, s_b^T) &\equiv \rho_T^{\text{pert}}(x; s) \frac{1}{2} [\theta(s_\rho^T - s) + \theta(s_b^T - s)]. \end{aligned} \quad (\text{B.16})$$

C Definition of χ^2 in the sum rules

Let us discuss the definition of χ^2 for the SR case. We have here the function $F(M^2, s)$, and the problem is to find the best value s_0 , such that $F(M^2, s_0)$ is the most

close to a constant value for $M_-^2 \leq M^2 \leq M_+^2$ (values of M_{\pm}^2 are known and fixed from standard constraints of QCD SR, see [30,8]). We define the function $\chi^2(s)$ for the curve $F(M^2, s)$ with $M^2 \in [M_-^2, M_+^2]$ in the following manner:

$$\chi^2(s) \equiv \frac{1}{(N-1)\epsilon^2} \sum_{k=0}^N [F(M_-^2 + k\delta, s) - \frac{1}{N+1} \sum_{k=0}^N F(M_-^2 + k\delta, s)]^2, \quad (\text{C.1})$$

where $\delta = (M_+^2 - M_-^2)/N$, $N \simeq 10$, and ϵ is of an order of the last decimal digit in $F(M^2, s)$ we are interested in (in the case of decay constant $f_\rho \approx 200$ MeV, $\epsilon \approx 1$ MeV; in the case of the second moment $\langle \xi^2 \rangle_\rho \approx 0.25$, $\epsilon \approx 0.01$). Then, if we obtain $\chi^2(s_0) \approx 1$, this tells us that the mean deviation of $F(M^2, s_0)$ from a constant value in the region $[M_-^2, M_+^2]$ is about ϵ . To find the minimum value of χ^2 and the corresponding s_0 , we used the code Mathematica.

References

1. V.L. Chernyak, A.R. Zhitnitsky, JETP Lett. **25**, 510 (1977); V.L. Chernyak, A.R. Zhitnitsky, V.G. Serbo, JETP Lett. **26**, 594 (1977); Stanley J. Brodsky, G. Peter Lepage, Phys. Lett. B **87**, 359 (1979); A.V. Efremov, A.V. Radyushkin, Phys. Lett. B **94**, 245 (1980)
2. V.L. Chernyak, A.R. Zhitnitsky, Nucl. Phys. B **201**, 492 (1982); B **214**, 547(E) (1983); Phys. Rept. **112**, 173 (1984)
3. J. Govaerts, L.J. Reinders, F. de Viron, J. Weyers, Nucl. Phys. B **283**, 706 (1987)
4. Patricia Ball, V.M. Braun, Phys. Rev. D **54**, 2182 (1996)
5. Patricia Ball, V.M. Braun, Y. Koike, K. Tanaka, Nucl. Phys. B **529**, 323 (1998)
6. S.V. Mikhailov, A.V. Radyushkin, JETP Lett. **43**, 712 (1986); Sov. J. Nucl. Phys. **49**, 494 (1989)
7. S.V. Mikhailov, A.V. Radyushkin, Phys. Rev. D **45**, 1754 (1992); A.P. Bakulev, A.V. Radyushkin, Phys. Lett. B **271**, 223 (1991)
8. A.P. Bakulev, S.V. Mikhailov, Phys. Lett. B **436**, 351 (1998)
9. A.V. Radyushkin, Talk given at ICTP Conference on Perspectives in Hadronic Physics, Trieste, Italy, 12–16 May, 1997 [hep-ph/9707335], pp. 1–10
10. V.M. Braun, I.E. Filyanov, Z. Phys. C **44**, 157 (1989)
11. N.G. Stefanis, W. Schroers, H.C. Kim, Phys. Lett. B **449**, 299 (1999)
12. A. Schmedding, O. Yakovlev, Phys. Rev. D **62**, 116002 (2000)
13. A.V. Radyushkin, in Workshop on Continuous Advances in QCD, Proceedings Workshop, Minneapolis, February 18–20, 1994 (University of Minnesota, Minneapolis, 1994), pp. 238–248
14. A.P. Bakulev, S.V. Mikhailov, Z. Phys. C **68**, 451 (1995); Mod. Phys. Lett. A **11**, 1611 (1996)
15. A.V. Radyushkin, R.T. Ruskov, Nucl. Phys. B **481**, 625 (1996)
16. A.P. Bakulev, S.V. Mikhailov, Eur. Phys. J. C **17**, 129 (2000)
17. S.V. Mikhailov, Phys. Atom. Nucl. **56**, 650 (1993)
18. A.G. Grozin, Int. J. Mod. Phys. A **10**, 3497 (1995)
19. V.M. Belyaev, B.L. Ioffe, Sov. Phys. JETP **57**, 716 (1983); A.A. Ovchinnikov, A.A. Pivovarov, Sov. J. Nucl. Phys. **48**, 721 (1988); A.A. Pivovarov, Bull. Lebedev Phys. Inst. **5**, 1 (1991)
20. M.V. Polyakov, C. Weiss, Phys. Lett. B **387**, 841 (1996); A.E. Dorokhov, S.V. Esaibegian, S.V. Mikhailov, Phys. Rev. D **56**, 4062 (1997)
21. M. D'Elia, A. Di Giacomo, E. Meggiolaro, Phys. Rev. D **59**, 054503 (1999); E. Meggiolaro, Nucl. Phys. Proc. Suppl. **83**, 512 (2000)
22. H.G. Dosch, M. Eidemüller, M. Jamin, E. Meggiolaro, JHEP **07**, 023 (2000)
23. D.E. Groom et al., Eur. Phys. J. C **15**, 1 (2000)
24. D. Becirevic et al., Nucl. Phys. Proc. Suppl. **73**, 222 (1999); [hep-lat/9809129]
25. M.V. Polyakov, Nucl. Phys. B **555**, 231 (1999)
26. A.P. Bakulev, S.V. Mikhailov, R. Ruskov, in Heavy Quark Physics, Proceedings 5th International Workshop, Dubna, Russia, 5–9 April 2000, edited by M.A. Ivanov, V.E. Lyubovitskij, E. Lipartia (Joint Institute for Nuclear Research, Dubna, 2000), pp. 31–35
27. Patricia Ball, V.M. Braun, Phys. Rev. D **55**, 5561 (1997)
28. Patricia Ball, V.M. Braun, Phys. Rev. D **58**, 094016 (1998)
29. T.M. Aliev, V.L. Eletsky, Sov. J. Nucl. Phys. **38**, 936 (1983); E. Bagan, Patricia Ball, V.M. Braun, H.G. Dosch, Phys. Lett. B **278**, 457 (1992)
30. M.A. Shifman, A.I. Vainshtein, V.I. Zakharov, Nucl. Phys. B **147**, 385 (1979), 448, 519
31. V.M. Belyaev, A. Oganesian, Phys. Lett. B **395**, 307 (1997)